

## Absolute generalized oscillator strengths for the vibronic bands of $A^1\Pi$ , $B^1\Sigma^+$ , $C^1\Sigma^+$ , and $E^1\Pi$ transitions of carbon monoxide

Z. P. Zhong, R. F. Feng, K. Z. Xu, S. L. Wu, L. F. Zhu, X. J. Zhang, Q. Ji, and Q. C. Shi

*Department of Modern Physics, University of Science and Technology of China, Hefei, Anhui, 230026, People's Republic of China*

(Received 15 July 1996; revised manuscript received 15 October 1996)

Generalized oscillator strengths for the vibronic bands of  $A^1\Pi$ ,  $B^1\Sigma^+$ ,  $C^1\Sigma^+$ , and  $E^1\Pi$  have been determined by an angle-resolved electron energy loss spectroscopy at an incident electron energy of 1500 eV and in an angular range of  $0.5^\circ$ – $6.0^\circ$ . The corresponding absolute optical oscillator strengths obtained by extrapolating the generalized oscillator strengths to  $K^2=0$  are also reported. The present results have been compared with previous work, and some differences between them have been explained. The experimental generalized oscillator strengths for  $v'=0-8$  of  $A^1\Pi$ ,  $v'=0-1$  of  $B^1\Sigma^+$ ,  $C^1\Sigma^+$ , and  $E^1\Pi$  are reported. [S1050-2947(97)00203-5]

PACS number(s): 33.70.Ca, 33.70.Fd

### I. INTRODUCTION

The investigation of the structure of atomic and molecular energy levels and electron-induced processes has been drawing increasing experimental and theoretical attention [1–5]. Absolute differential cross sections (DCSs) for electronic excitations in carbon monoxide are of undisputed interest in atmospheric and plasma physics since carbon monoxide is an important component in the atmosphere and interstellar medium. Most previous experimental studies of electron-induced processes of carbon monoxide have been devoted to measurements of DCSs at low impact energies ( $\leq 100$  eV), and have been quoted in Ref. [6]. DCSs of carbon monoxide at intermediate or high impact energy have only been measured by Lassetre and co-workers [7–10] for  $v'=2$  of  $A^1\Pi$ ,  $v'=0$  of  $B^1\Sigma^+$  and  $C^1\Sigma^+$ . The corresponding generalized oscillator strengths (GOSs) have been determined from the measured DCSs. Theoretical calculations for the vibronic bands of  $A^1\Pi$ ,  $B^1\Sigma^+$ ,  $C^1\Sigma^+$ , and  $E^1\Pi$  have recently been reported by Chantranupong *et al.* [11,12]. However, the differences between their calculations and the GOSs measured by Lassetre and co-workers [7–10] are larger for both the values and the profiles of GOS curves. Up to now, there have only been theoretical calculations for the GOSs of  $v'=1$  of  $B^1\Sigma^+$  and  $C^1\Sigma^+$ , and  $v'=0$ , 1 of  $E^1\Pi$ .

The existing values of absolute optical oscillator strengths (OOSs) in the discrete region for carbon monoxide show large differences among the various experimental and theoretical works. The difficulties and limitations for optical methods in determining OOSs for discrete transitions have been discussed in Refs. [3,13]. There are only three groups which have applied electron impact methods based on electron energy loss spectroscopy (EELS) to determine OOSs for discrete transitions of carbon monoxide. Lassetre and Skerbele [9] have obtained the OOS values for  $v'=2$  of  $A^1\Pi$  by extrapolating a series of GOSs to zero momentum transfer square ( $K^2$ ) and normalizing their relative data on the absolute elastic differential cross sections measured by Bromberg [14]. The absolute OOSs for the vibronic bands of the  $B^1\Sigma^+$ ,  $C^1\Sigma^+$ , and  $E^1\Pi$  excited states have been deter-

mined from the height ratios of the corresponding peaks to  $v'=2$  of  $A^1\Pi$  in a spectrum measured at  $0^\circ$  angle. Chan *et al.* [15] and Wu *et al.* [16] have employed a high-resolution dipole ( $e,e$ ) method to directly determine the OOSs for the vibronic bands of the  $A^1\Pi$ ,  $B^1\Sigma^+$ ,  $C^1\Sigma^+$ , and  $E^1\Pi$ , in which the optical limit (i.e.,  $K^2 \rightarrow 0$ ) are effectively satisfied. The OOSs for the vibronic bands of the  $A^1\Pi$  obtained by each group are consistent. However, the OOSs reported by Lassetre and Skerbele [9] for the vibronic bands of the  $B^1\Sigma^+$ ,  $C^1\Sigma^+$ , and  $E^1\Pi$  show large deviations from the data of Chan *et al.* [15] and Wu *et al.* [16]. On the other hand, the data of Chan *et al.* [15] are in good agreement with those of Wu *et al.* [16] for these vibronic bands.

In this paper our experimental results for the GOSs of the vibronic bands of the  $A^1\Pi$ ,  $B^1\Sigma^+$ ,  $C^1\Sigma^+$ , and  $E^1\Pi$  electronic states are reported at an incident electron energy of 1500 eV and in an angular range of  $0.5^\circ$ – $6.0^\circ$  with an interval of  $0.5^\circ$ . The OOSs for  $B^1\Sigma^+$ ,  $C^1\Sigma^+$ , and  $E^1\Pi$  are also obtained by extrapolating the GOSs to  $K^2=0$ . Moreover, we try to explain the differences among the OOS of  $B^1\Sigma^+$ ,  $C^1\Sigma^+$ , and  $E^1\Pi$  reported by Lassetre and Skerbele [9], Wu *et al.* [16], and Chan *et al.* [15].

### II. EXPERIMENTAL METHOD

According to the Bethe theory [1,17], the differential cross section per unit range of  $E$ ,  $d^2\sigma(K,E)/dEd\Omega$ , for a fast electron impact can be factored into two parts involving the kinematics of the electron before and after collision, and the transition probability of the resulting excitation of target, the so-called generalized oscillator strength density  $df/dE$ , by the following Bethe-Born formula:

$$\frac{df(K,E)}{dE} = \frac{E}{2} K^2 \frac{p_o}{p_a} \frac{d^2\sigma(K,E)}{dEd\Omega}. \quad (1)$$

Here  $E$  and  $K$  stand for energy loss and momentum trans-

fer while  $p_o$  and  $p_a$  are incident and scattered electron momenta, respectively. All quantities in Eq. (1) and following equations are in atomic units.

It can also be shown [1,17] that the generalized oscillator strength density can be expanded in a power series of  $K^2$  as

$$\frac{df(K,E)}{dE} = \frac{df_o(E)}{dE} + AK^2 + BK^4 + \dots, \quad (2)$$

where  $df_o(E)/dE$  is the optical oscillator strength density and  $A, B$ , etc. are constants. Therefore at the optical limit (i.e.,  $K^2 \rightarrow 0$ ), it will be found that

$$\lim_{K^2 \rightarrow 0} \frac{df(K,E)}{dE} = \frac{df_o(E)}{dE}. \quad (3)$$

Under such conditions of negligible momentum transfer, the dipole selection rules are applicable and

$$\frac{df_o(E)}{dE} = \frac{E}{2} K^2 \frac{p_o}{p_a} \frac{d^2\sigma(K,E)}{dEd\Omega} = B(E) \frac{d^2\sigma(E)}{dEd\Omega}. \quad (4)$$

The quantity  $B(E)$  is called the Bethe-Born factor. In an actual experiment, the factor  $B(E)$  must take into account the finite acceptance angle about the mean scattering angle of  $0^\circ$  and the energy-dependent efficiency factor. Therefore Eq. (4) can be modified to give [18]

$$\frac{df_o(E)}{dE} = B'(E) \frac{dN(E)}{dE},$$

$$B'(E) = \frac{df_o(E)/dE}{dN(E)/dE} = \frac{E}{a+cE} \ln^{-1} \left( 1 + \frac{\theta_0^2}{x^2} \right). \quad (5)$$

$dN(E)/dE$  is measured counts per unit range of  $E$  in the measured electron energy loss spectrum.  $B'(E)$  is called the Bethe-Born conversion factor, which can be obtained by referencing a high-resolution electron energy loss spectrum to the known photoabsorption cross section in the smooth ionization continuum spectral region of a suitable gas (such as helium). Here  $x = E/2E_0$  ( $E_0$  is the impact energy),  $\theta_0$  is the half acceptance angle of the analyzer. Values of  $a, c$ , and  $\theta_0$  can be determined from a least-squares fit.

It is well known that the electron impact methods based on EELS for determining optical oscillator strengths can be briefly classified into two types [3].

(1) An extrapolating EELS method, pioneered in the 1960s by Lassette and co-workers, such as in Refs. [7–10]. This method involves measurements of the relative intensity for a given transition as a function of scattering angles (i.e.,  $K^2$ ) [see Eqs. (1)–(3)] which can be extrapolated to  $K^2 = 0$  to give the relative OOS for this transition. The GOSs determined in the series of measurements have an important role for investigating electron-induced processes. In addition, such information is also a crucial requirement for the development and evaluation of quantum-mechanical theoretical methods and for the various modeling procedures involving electronic transition probabilities, since a profile of the GOS versus  $K^2$  curve is directly related to the initial-state and excited-state wave functions. Meanwhile, intensity ratios determined as a function of scattering angle, which are the

products of the series of measurements, are useful in the study of intensity distribution among vibronic levels in electronic transitions and in the identification of forbidden transitions [19].

When the incident electron energy is sufficiently high, the measured apparent GOS will tend to the GOS calculated from Eq. (1) relying on the first Born approximation. But previous experiments were operated at a typical impact energy of 500 eV, which is not high enough for this. Lassette, Skerbele, and Dillon [20] have conjectured through some modeling and/or intuition that the limiting oscillator strength at  $K^2 = 0$  is the optical oscillator strength in the case of optically (dipole) allowed transitions, regardless of whether the first Born approximation holds or not [Eq. (1) depends on the use of the first Born approximation and hence holds only at high energy], which is called the theory of limiting oscillator strengths. This conjecture was based on a great deal of experimental evidence, and it is a useful tool for experimental work. The Lassette formula has been extensively used to fit the experimental data to obtain the OOS [20]:

$$f(K, E_0) = \frac{1}{(1+y)^6} \left[ f_o + \sum_{k=1}^m f_k \left( \frac{y}{1+y} \right)^k \right], \quad (6)$$

where  $y = K^2/\alpha^2$ ,  $\alpha = (2I)^{1/2} + [2(I-E)]^{1/2}$ , and  $I$  is the ionization potential,  $f_o$  is OOS, and  $f_k$  are fitted constants.

(2) Dipole ( $e, e$ ) method which is a direct method to determine OOS and has been described in detail in Ref. [3]. Briefly, it avoids the need for the extrapolation procedure by choosing a series of experimental conditions, in which the optical limit (i.e.,  $K^2 \rightarrow 0$ ) is effectively satisfied [21–23]. This can be achieved by measuring at high impact energy  $E_0$  and designing the electron analyzer and associated electron optics so that the measurement can be done at a mean scattering angle of  $0^\circ$ . This usually results in  $K^2 < 0.01$  a.u. for valence electron excitations and fast electron impact. Under such conditions, Eq. (4) is satisfied to better than 1% accuracy for most cases. It should be noticed that the formula of  $B'(E)$  in Eq. (5) has assumed  $df_o(E)/dE$  as a constant within the angle range from  $-\theta_0$  to  $+\theta_0$ . The errors resulting from this assumption are negligible for most transitions (less than 1%). But it has been found that some forbidden transitions have been detected in experiment where the optical limit is satisfied, for example, in Refs. [24–26]. Obviously, the dipole ( $e, e$ ) method cannot directly identify the forbidden transition well.

A further development of high-energy-resolution fast EELS is angle-resolved EELS (AREELS), in which the optical limit is effectively satisfied at a mean scattering angle of  $0^\circ$ , and the scattering angle can be varied. So AREELS can be applied to measure directly absolute OOSs for dipole electronic transitions and absolute DCSs and GOSs for both dipole and nondipole electronic transitions. Therefore the AREELS can compare the dipole ( $e, e$ ) EELS method with the extrapolating EELS method for determining OOSs and can be used to test the theory of limiting oscillator strengths [20]. Details of the apparatus were described in our previous work [24,27]. Briefly it consists of an electron gun, a hemispherical electrostatic monochromator made of aluminum, a rotatable energy analyzer of the same type, an interaction chamber, a number of cylindrical electrostatic optics lenses,

and a channeltron for detecting the analyzed electrons. All of these components are enclosed in four separate vacuum chambers made of stainless steel. Pulse-counting and multi-scaler techniques were used to obtain energy loss spectra. The impact energy of the spectrometer can be varied from 1 keV to 5 keV and the energy resolution is 40–120 meV [full width at half maximum (FWHM)]. The background pressure in the vacuum chambers was  $3.0 \times 10^{-5}$  Pa. The scattering angles were calibrated based on the symmetry of the electronic transition  $A^1\Pi$  around the geometric zero angle. The angular resolution of the spectrometer has been approximately determined from the angular distribution of the direct electron beam from the monochromator measured by rotating the analyzer, and it is about  $0.8^\circ$  (FWHM) in the present measurements. The impact energy was set at 1.5 keV and the energy resolution was about 50 meV to 70 meV for the present measurements.

There were some small variations in the intensity of the incident electron beam during the measuring period. In order to minimize this systematic error, elastic, inelastic, then elastic EELS spectra were measured at an angle for each cycle and an elastic EELS spectrum at an angle of  $4.0^\circ$  was measured before and after this cycle. Every measured count of both elastic and inelastic scattering was normalized to that of elastic intensity at  $4.0^\circ$ . Double scattering processes can cause errors in DCS measurements of inelastic scattering [28]. The double scattering effect has been evaluated and corrected in this work for scattering angles not smaller than  $2.0^\circ$ . The method is described in Refs. [4,29]. Briefly, the pressure relation of the intensity ratios of inelastic scattering to elastic scattering at the same scattering angles ( $\geq 2.0^\circ$ ) was measured. There is an approximate relation between the measured intensity ratios and the pressure  $p$  as follows:

$$\frac{I_p(\theta)}{I_{el}(\theta)} = \left( \frac{I_p(\theta)}{I_{el}(\theta)} \right)_{p=0} + C(\theta)p, \quad (7)$$

where  $I_p$  and  $I_{el}$  represent the scattering intensities corresponding to the inelastic scattering and elastic scattering, respectively, which include single and double scattering. In this experiment, we have measured the intensity ratios at five pressures: 0.008, 0.015, 0.020, 0.025, and 0.030 Pa.  $[I_p(\theta)/I_{el}(\theta)]_{p=0}$  is the intensity ratio extrapolating to zero gas pressure which is a real relative inelastic scattering intensity ratio without the pressure effect. Therefore after the least-squares fit was employed to fit the data points according to Eq. (7), the double scattering effect was evaluated and corrected.

In the collision cell case, the scattered electrons go out not from a point, but from a line. The scattering length “seen by” the energy analyzer at a scattering angle  $\theta$  is proportional to  $1/\sin\theta$  at larger scattering angles. But at smaller scattering angles it does not increase further because of the fixed length of the collision cell. In the present work, we adopted the method in Ref. [4] for calibrating the angular factor of our apparatus to correct the line source and other effects. Briefly, our angular factor  $A(\theta)$  was obtained by dividing the DCS values of the  $1^1S \rightarrow 2^1P$  transition of helium obtained from Kim and Inokuti [30] by the measured counts for the transition  $1^1S \rightarrow 2^1P$  of helium at different angles and the results being normalized at an angle of  $4.0^\circ$ .

In this work we extrapolated the relative GOSs of  $v'=2$  of  $A^1\Pi$  to  $K^2=0$  using Eq. (6) to obtain its relative OOS, then normalized the relative OOS to the absolute OOS (0.0401) measured by Wu *et al.* [16] and made its GOSs absolute. The other sets of relative GOSs were made absolute by reference to concurrent measurements of the absolute GOS  $v'=2$  of  $A^1\Pi$  at the same angle or fitted values at  $0.5^\circ$ ,  $1.0^\circ$ , and  $1.5^\circ$ .

### III. RESULTS AND DISCUSSIONS

Figures 1(a)–1(c) show the EELS spectra measured at scattering angles  $0^\circ$ ,  $3^\circ$ , and  $6^\circ$ , respectively, which were measured at the gas pressure of 0.008 Pa. For the partially resolved peaks, a Fourier self-deconvolution method, which has been successfully used in Ref. [31], has been employed to determine the intensities of the respective peaks shown in Figs. 1(a)–1(c).

Figure 2(a) shows the pressure relation of the intensity ratios of  $v'=2$  of  $A^1\Pi$  to elastic scattering at the same scattering angle. It is obvious that  $C(\theta)$  changes with the scattering angle. For example, at the pressure of 0.008 Pa, the difference between the DCS before and after the double scattering effect has been corrected by Eq. (6) is 1% at  $2.0^\circ$ , but it becomes 34% at  $6.0^\circ$ . The pressure relations of the intensity ratios of the other vibronic bands have the same situation as  $v'=2$  of  $A^1\Pi$ . Figure 2(b) shows the relationships between  $C(\theta)$  and  $\theta$  for  $v'=2$  of  $A^1\Pi$ ,  $v'=0$  of  $B^1\Sigma^+$ ,  $v'=0$  of  $C^1\Sigma^+$ , and  $v'=0$  of  $E^1\Pi$ . Obviously, these relationships have an approximately linear relationship for the above vibronic states.

Subtracting backgrounds, correcting with the instability of beam current and the effect of double scattering processes, and multiplying the corresponding angular factors  $A(\theta)$  at every scattering angle, the relative DCSs and GOSs for the vibronic states of  $A^1\Pi$ ,  $B^1\Sigma^+$ ,  $C^1\Sigma^+$ , and  $E^1\Pi$  were obtained. The overall percent error of the GOSs obtained in the present work mainly comes from instability of beam current, the pressure correction, the angular determination, the angular correction factor, the statistics of counts, and the systematic error from measuring the OOS of  $v'=2$  of  $A^1\Pi$ , as well as the error resulting from the deconvoluting procedure. The largest error is less than 10% for  $v'=0-6$  of  $A^1\Pi$ ,  $v'=0$  of  $B^1\Sigma^+$ ,  $v'=0$  of  $C^1\Sigma^+$ , and  $v'=0$  of  $E^1\Pi$ , less than 15% for  $v'=7-8$  of  $A^1\Pi$ ,  $v'=1$  of  $C^1\Sigma^+$ , and  $v'=1$  of  $E^1\Pi$ , and less than 20% for  $v'=1$  of  $B^1\Sigma^+$ .

#### A. Relative intensities within the vibronic progressions of $A^1\Pi$ , $B^1\Sigma^+$ , $C^1\Sigma^+$ , and $E^1\Pi$

Over a long period of time, it has been assumed in the application of EELS, such as in Refs. [7–10,31], that the intensity distribution of vibronic band in a molecular electronic transition remains constant, regardless of scattering angle and incident electron energy, i.e., the Franck-Condon principle. Lassette and co-workers, as in Refs. [7–10], have studied some molecules to confirm the Franck-Condon principle by measuring the relative intensities of a few well separated vibronic progressions as a function of scattering angles. However, Klump and Lassette [32,33] noted a breakdown of this rule in  $B^1\Sigma^+ \leftarrow X^1\Sigma^+$  in CO and  $B'^3\Sigma_u^+ \leftarrow X^3\Sigma_g^+$  in

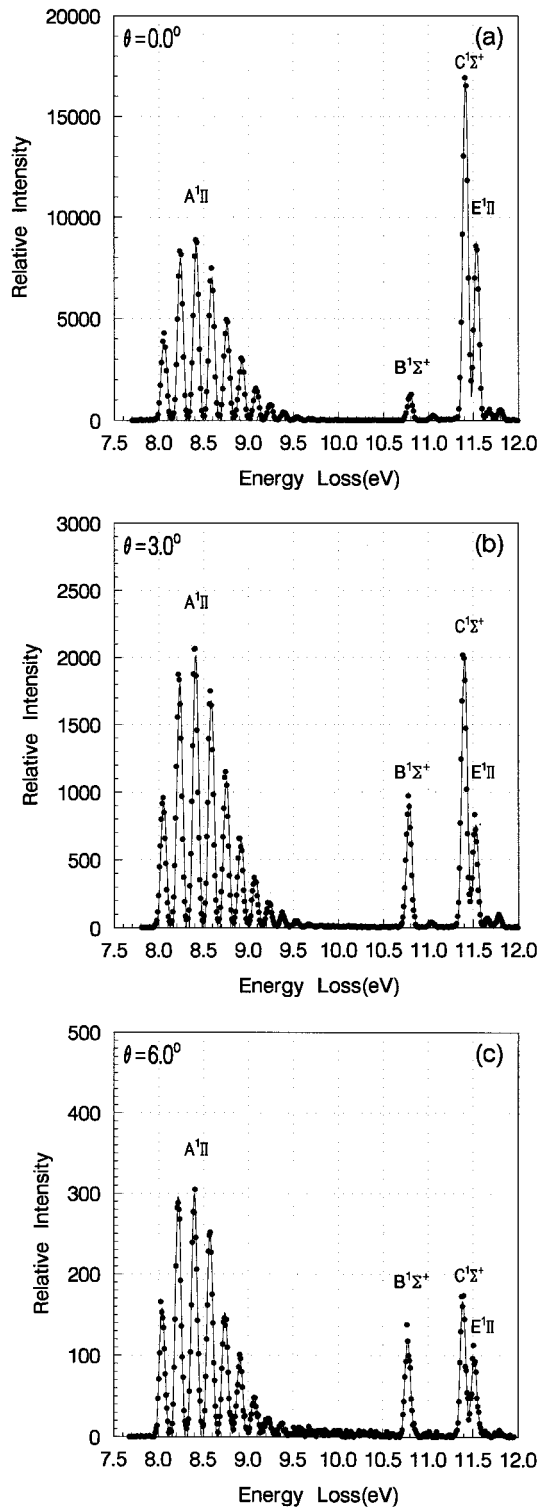


FIG. 1. Electron energy loss spectra for carbon monoxide at 1500 eV impact energy. The deconvoluted peaks are plotted as solid lines. (a) Scattering angle at  $0.0^\circ$ . (b) Scattering angle at  $3.0^\circ$ . (c) Scattering angle at  $6.0^\circ$ .

$O_2$ . Figure 3 shows our results in this work and previous data for the vibronic bands of  $A^1\Pi$ ,  $B^1\Sigma^+$ ,  $C^1\Sigma^+$ , and  $E^1\Pi$ . Certainly, our results about  $A^1\Pi$  are in agreement with the data of Lassette and Skerbele [9] within experimental error. Figure 3(a) only shows the intensity ratio of  $v'=1$  to  $v'=0$  of  $A^1\Pi$  and indicates the intensity ratio

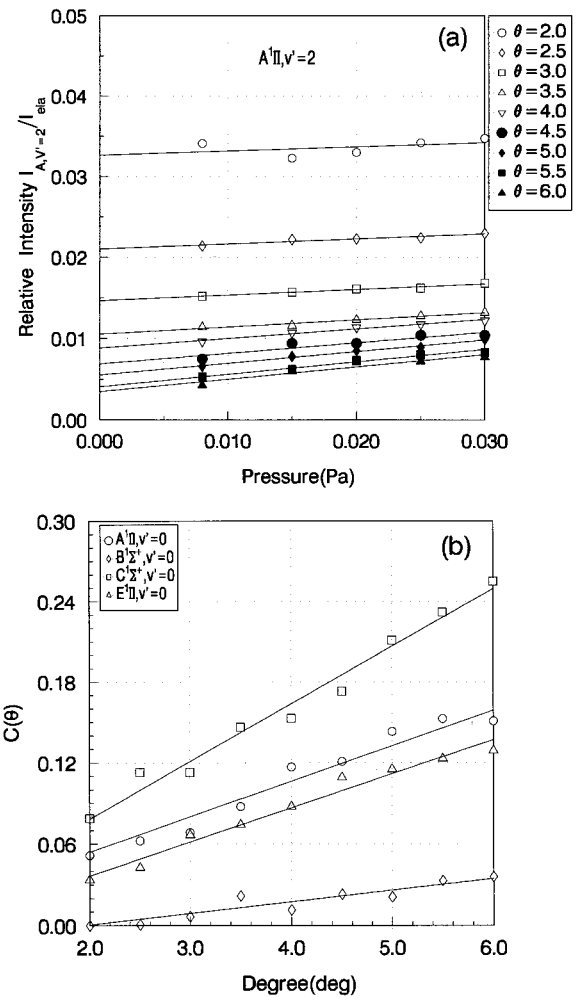


FIG. 2. (a) Intensity ratios  $I_p/I_{el}$  as a function of pressure for  $v'=2$  of  $A^1\Pi$ . (b) The relationship between  $C(\theta)$  and scattering angle  $\theta$  for  $v'=2$  of  $A^1\Pi$ ,  $v'=0$  of  $B^1\Sigma^+$ ,  $C^1\Sigma^+$ , and  $E^1\Pi$ .

remains constant within the scattering angle range in this work.  $v'=0,3-8$  of  $A^1\Pi$  have the same situation as that of  $v'=1$ . The breakdown of the Franck-Condon principle in  $B^1\Sigma^+ \leftarrow X^1\Sigma^+$  has also been observed as in Fig. 3(b), although the error of relative intensity ratio of  $v'=1$  of  $B^1\Sigma^+$  to  $v'=0$  of  $B^1\Sigma^+$  is large, nevertheless it is far from constant, changing by a factor of 2 over the momentum transfer range of 0.4 a.u. (i.e., angular range from  $1.5^\circ$  to  $3.5^\circ$ ). Theoretical values [12] about  $B^1\Sigma^+ \leftarrow X^1\Sigma^+$  also indicate breakdown of the Franck-Condon principle. The reason for the anomalous  $B-X$  behavior of CO has been explained by Dillon *et al.* [34] for the presence of an avoided crossing. The data for  $C^1\Sigma^+$  and  $E^1\Pi$  in this work are reported experimentally. The variations of the intensity ratios within vibrational progressions of  $C^1\Sigma^+$  and  $E^1\Pi$  shown in Figs. 3(c) and 3(d) are not as dramatic as in the case of  $B^1\Sigma^+$ . However, the largest differences for  $C^1\Sigma^+$  and  $E^1\Pi$  exceed experimental error. Theoretical values [12] for  $C^1\Sigma^+$  and  $E^1\Pi$  have also shown variation of the Franck-Condon envelope with momentum transfer.

### B. The GOSs for $v'=0-8$ of $A^1\Pi$

Although there are considerable discrepancies among the OOS values for carbon monoxide corresponding to electron

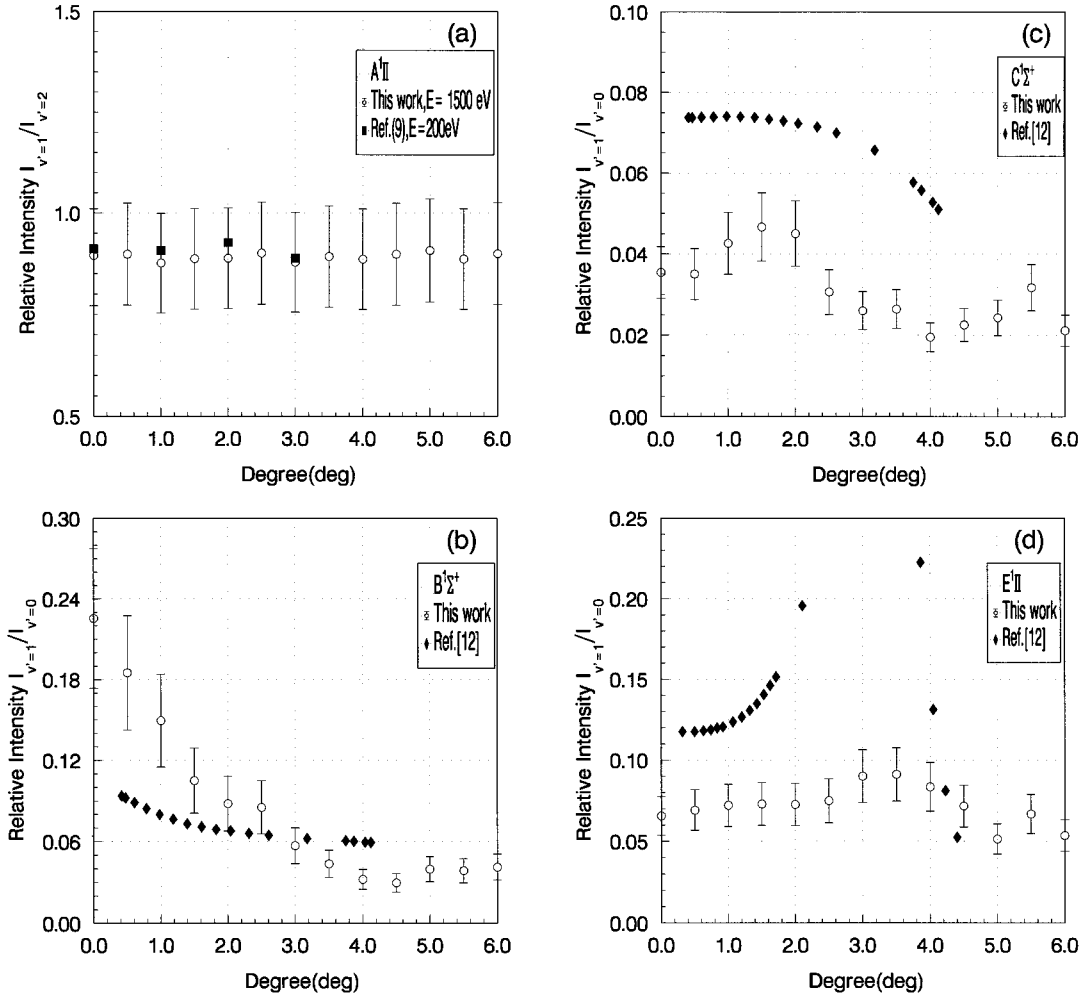


FIG. 3. (a) Intensity ratio of  $v'=1$  to  $v'=0$  of  $A^1\Pi$  as a function of scattering angle  $\theta$ . (b) Intensity ratio of  $v'=1$  to  $v'=0$  of  $B^1\Sigma^+$  as a function of scattering angle  $\theta$ . (c) Intensity ratio of  $v'=1$  to  $v'=0$  of  $C^1\Sigma^+$  as a function of scattering angle  $\theta$ . (d) Intensity ratio of  $v'=1$  to  $v'=0$  of  $E^1\Pi$  as a function of scattering angle  $\theta$ .

impact [9,15,16], optical measurements [35–38], and the theoretical calculations, the OOSs for the  $A$ - $X$  valence band system are almost in agreement with each other. Moreover, three GOS versus  $K^2$  curves for  $v'=2$  of  $A^1\Pi$  at impact energy 300, 400, and 500 eV measured by Lassette and Skerbele [9] fall on the same curve within experimental error, which indicates that the first Born approximation holds in their measurements, and their GOSs for  $v'=2$  of  $A^1\Pi$  should equal the data calculated from the first Born approximation. The absolute GOSs for  $v'=2$  of  $A^1\Pi$  have been obtained in this work by extrapolating the relative GOSs to  $K^2=0$  according to Eq. (6) and using the absolute OOS value (0.0401) measured by Wu *et al.* [16]. In using Eq. (6), Lassette and Skerbele [39] showed that the choice of  $m$  was somewhat subjective and generally varied from 2 to 5, so the values of the coefficients  $f_k$  in Eq. (6) were somewhat arbitrary. In order to reduce the subjectivity in the choice of  $m$  in using Eq. (6), Ying *et al.* [40] have restricted the number of terms in Eq. (6) to four (i.e.,  $m=3$ ). In this paper we put forward some conditions to restrict the choice of  $m$ . Generally, if these conditions are satisfied, the value of  $m$  has a unique value.

(1) From the mathematics point of view, the sum of weighted square residual errors, i.e.,  $\chi^2$ , for a least-squares curve fitting procedure should be small, while it should not deviate too much from the value of  $n - m - 1$ , where  $n$  is the number of fitted GOSs. A suitable value of  $m$  can realize this requirement.

(2) It was found [40] that if  $m$  was increased, the absolute errors of the fitted coefficients  $f_k$  become much larger, so the values of  $f_k$  became more unreliable. Therefore one should choose the value of  $m$  to satisfy (1) and make the relative errors of  $f_k$  small as far as possible.

The above rules have been employed in this work. It is interesting that all the values of  $m$  for  $v'=0-8$  of  $A^1\Pi$  are equal to 0. Figure 4(a) shows the present GOS versus  $K^2$  curve for  $v'=2$  of  $A^1\Pi$  and previous data [9]. It is clear the profile of the GOS versus  $K^2$  curve reported by Chantran-pong *et al.* [12] for  $v'=2$  of  $A^1\Pi$  is similar to our result. Furthermore, the calculated GOSs for  $v'=2$  of  $A^1\Pi$  will be in good agreement with our results if their calculated OOS was 0.00401. While the data obtained by Lassette and Skerbele [9] show slight discrepancies compared with our results and theoretical calculations in terms of the profile of the

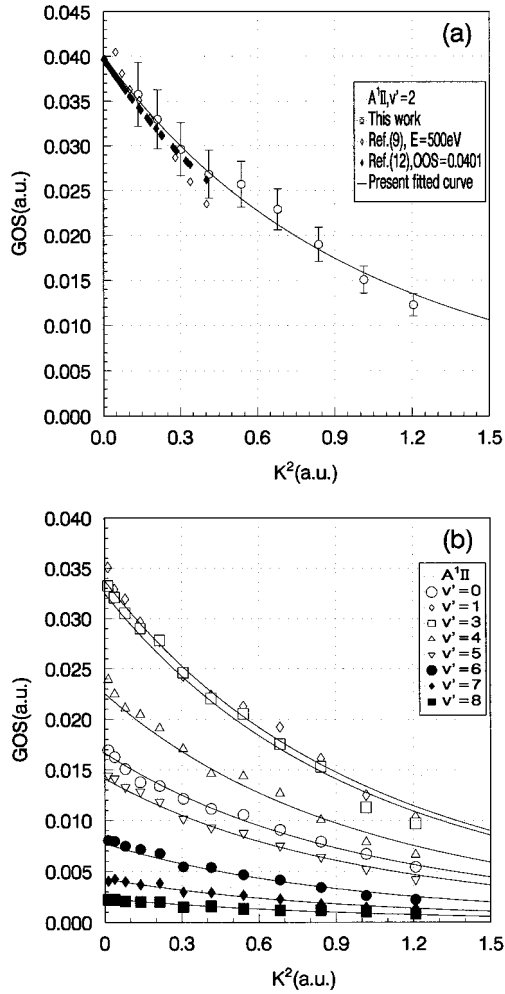


FIG. 4. (a) Absolute GOSs for  $v'=2$  of  $A^1\Pi$  as a function of  $K^2$ . (b) Absolute GOSs for  $v'=0,1,3-8$  of  $A^1\Pi$  as a function of  $K^2$ .

GOS versus  $K^2$  curves, they are consistent with our data within experimental errors. For  $v'=0,1,3-8$  of  $A^1\Pi$ , the situations are the same as  $v'=2$  of  $A^1\Pi$  compared with the calculated data of Chantranupong *et al.* [12] and shown in Fig. 4(b).

The OOSs in this work obtained by extrapolating the GOSs to  $K^2=0$  for  $v'=0-8$  of  $A^1\Pi$  and other previous data are presented in Table I. Clearly, our results in the present work are consistent with the other data based on

EELS methods within experimental error whether the extrapolating EELS method [9] or the dipole ( $e,e$ ) method [15,16] was employed, although the data of Lassetre and Skerbele [9] are generally larger than those of the present work. Compared with optical measurements [35,36], they are also in agreement with each other. The theoretical data calculated by Kirby and Cooper [41] are generally lower than the present data by 5–10%, but they are in agreement within experimental error. The calculated results of Chantranupong *et al.* [11] show much greater discrepancies with the present work, in terms of both the absolute magnitudes of the oscillator strengths and the profile of the vibrational envelope of the band.

### C. The GOSs of $v'=0-1$ of $B^1\Sigma^+$ , $C^1\Sigma^+$ , and $E^1\Pi$

Lassetre [42] has devoted some discussions to the fact that there are theoretical grounds for expecting that the first Born approximation should not hold for transitions between states possessing the same spatial symmetry, such as  $B^1\Sigma^+ \leftarrow X^1\Sigma^+$  and  $C^1\Sigma^+ \leftarrow X^1\Sigma^+$ . In fact, Skerbele and Lassetre [10] have measured the generalized oscillator strengths (GOSs) for two transitions  $v'=0$  of  $B^1\Sigma^+ \leftarrow X^1\Sigma^+$  and  $C^1\Sigma^+ \leftarrow X^1\Sigma^+$  in carbon monoxide at impact energy of 300, 400, and 500 eV. These GOS versus  $K^2$  curves at these three impact energies fall on separate curves, while the three corresponding curves for  $v'=2$  of  $A^1\Pi$  fall on the same curve within experimental error [9]. Chantranupong *et al.* [12] have calculated the GOSs as a function of  $K^2$  for  $A-X$ ,  $B-X$ ,  $C-X$ , and  $E-X$  transitions of carbon monoxide, and have employed multireference configuration-interaction (CI) methods within the framework of the first Born approximation. The profiles of the calculated GOS versus  $K^2$  curves for the  $A-X$  and  $C-X$  transitions exhibit an appearance similar to the results observed by Lassetre and Skerbele [9,10], although the absolute magnitudes are different. However, the minimum in the observed  $v'=0$  of  $B^1\Sigma^+$  data [10] is not reproduced in the theoretical results. The previous GOSs for  $E-X$  have only theoretical values. Moreover, there are considerable discrepancies among electron impact [9,15,16] and optical measurements [38,39] for absolute OOSs of  $B^1\Sigma^+$ ,  $C^1\Sigma^+$ , and  $E^1\Pi$ . Even for the data based on electron methods, the data of Lassetre and Skerbele [9] are much larger than the data measured by Wu *et al.* [16] and Chan *et al.* [15] using the dipole ( $e,e$ ) method while the data of Wu *et al.* [16] are consistent with those of Chan *et al.* [15]. For the  $A-X$  transitions, they are

TABLE I. Absolute optical oscillator strengths for  $v'=0-8$  of  $A^1\Pi$  ( $\times 10^{-2}$ ).

$v'$	This work	Ref. [9]	Ref. [16]	Ref. [15]	Ref. [35]	Ref. [36]	Ref. [11]	Ref. [41]
0	1.66	2.00	1.78	1.62	1.65	1.56	1.48	1.55
1	3.38	3.80	3.56	3.51	3.37	3.43	3.56	3.24
2		4.29	4.01	4.02	4.24	4.12	4.73	3.73
3	3.25	3.60	3.40	3.47	3.77	3.61	4.62	3.16
4	2.25	2.51	2.45	2.42	2.58	2.58	3.71	2.20
5	1.41	1.55	1.53	1.45	1.63	1.61	2.62	1.34
6	0.77	0.848	0.78	0.805	1.04	0.91	1.68	0.75
7	0.43	0.437	0.41	0.414	0.59	0.48	0.10	0.39
8	0.23	0.217	0.22	0.202	0.29	0.24		0.19

TABLE II. The absolute generalized oscillator strengths for  $v'=0-1$  of  $B^1\Sigma^+$ ,  $C^1\Sigma^+$ , and  $E^1\Pi(\times 10^{-2})$ .

Angle ( $^\circ$ )	$B^1\Sigma_{v'=0}^+$	$B^1\Sigma_{v'=1}^+$	$C^1\Sigma_{v'=0}^+$	$C^1\Sigma_{v'=1}^+$	$E^1\Pi_{v'=0}$	$E^1\Pi_{v'=1}$
0.5	0.744	0.132	10.757	0.387	5.807	0.413
1.0	0.829	0.120	10.157	0.443	5.536	0.409
1.5	1.222	0.124	9.682	0.462	4.792	0.358
2.0	1.503	0.128	8.643	0.398	3.987	0.297
2.5	1.623	0.134	6.615	0.207	3.179	0.244
3.0	1.612	0.089	3.996	0.106	1.461	0.134
3.5	1.582	0.067	2.972	0.080	1.069	0.100
4.0	1.518	0.047	2.025	0.040	0.596	0.051
4.5	1.283	0.037	1.457	0.034	0.375	0.028
5.0	1.034	0.040	0.720	0.018	0.229	0.012
5.5	0.818	0.031	0.589	0.019	0.140	0.010
6.0	0.654	0.026	0.150	0.003	0.362	0.020

generally in good agreement among the various experimental and theoretical treatments. The theory of limiting oscillator strengths has illustrated that the limiting oscillator strength at  $K^2=0$  is the optical oscillator strength, regardless of whether the first Born approximation holds or not, which means that an OOS obtained by extrapolating the GOS to zero momentum transfer at various impact energies or by the dipole ( $e, e$ ) method should be in agreement with each other and be equal to the OOS determined by various optical measurements. Therefore the GOS measurements for  $v'=0-1$  of  $B^1\Sigma^+$ ,  $C^1\Sigma^+$ , and  $E^1\Pi$  at high electron impact energy should be useful to explain the above discrepancies among experimental and theoretical data for the values of GOSs and OOSs of  $v'=0-1$  of  $B^1\Sigma^+$ ,  $C^1\Sigma^+$ , and  $E^1\Pi$ .

The present absolute GOSs for  $B$ - $X$ ,  $C$ - $X$ , and  $E$ - $X$  transitions have been obtained by the method as used in  $A$ - $X$  transitions and have been listed in Table II and shown in Figs. 5(a)–5(d).

Figures 5(a) and 5(c) clearly show that the experimental GOS versus  $K^2$  curves obtained at 300, 400, 500, and 1500 eV for  $v'=0$  of  $B^1\Sigma^+$  and  $C^1\Sigma^+$  fall on separate curves and GOSs become larger with increasing electron impact energy. It indicates that the first Born approximation does not hold up to the impact energy equal of 500 eV, and the first Born approximation calculations for the above transitions should not be smaller than the present results. In fact, the corresponding calculations [12] relying on the first Born approximation for  $v'=0$  of  $B^1\Sigma^+$  are higher than these results, but the corresponding calculated data [12] for  $v'=0$  of  $C^1\Sigma^+$  are almost half of our results. There are no previous experimental data for  $v'=1$  of  $B^1\Sigma^+$  and  $C^1\Sigma^+$  and  $v'=0-1$  of  $E^1\Pi$ ; it can be expected that the first Born approximation for  $v'=1$  of  $B^1\Sigma^+$  and  $C^1\Sigma^+$  should not hold according to the theory of Lassetre [42].

The profile of the GOS curve calculated by Chantranupong *et al.* [12] for  $v'=0$  of  $B^1\Sigma^+$  has no minimum, which was observed by Skerbele and Lassetre [10]. However, it has been found in Fig. 5(a) that the minimum does not surely exist within experimental errors in this work, although the GOS (0.00744) at  $0.5^\circ$  is smaller than the OOS (0.00814) measured by Wu *et al.* [16] using the dipole ( $e, e$ ) method. Similarly, the situations of Skerbele and Las-

setre [10] at 300, 400, and 500 eV are the same as this work if the data at  $0.0^\circ$  are not included, because their data at  $0.0^\circ$  are unreliable (this will be illustrated later). The reason that the present OOS of  $v'=0$  of  $B^1\Sigma^+$  is larger than the present GOS at  $0.5^\circ$  may partly result from the finite acceptance angle  $\theta_0$ . As indicated above, the dipole ( $e, e$ ) method has assumed  $df(E)/dE$  as a constant within the angle range from  $-\theta_0$  to  $+\theta_0$ , the errors resulting from the assumption mainly influence those transitions whose GOSs change dramatically with  $K^2$  at small  $K^2$ . The fact that those dipole forbidden but quadrupole allowed transitions in Refs. [24–26] have been detected in zero angle EELS spectra, whose impact energies are larger and equal to 2.5 keV, may partly be due to this assumption. It should be noticed that the profile of the GOS versus  $K^2$  curve for  $v'=0$  of  $B^1\Sigma^+$  is not similar to a profile of a dipole allowed transition and its GOSs become small with decreasing  $K^2$  at small  $K^2$ , therefore if the minimum does not exist, it may not be surprising that the OOS for  $v'=0$  of  $B^1\Sigma^+$  obtained in this work by extrapolating the GOSs to  $K^2=0$  is smaller than the data measured by Wu *et al.* [16] and Chan *et al.* [15] using the dipole ( $e, e$ ) method. Our GOSs for  $v'=0$  of  $B^1\Sigma^+$  should be much closer to the first Born approximation calculations compared with the data of Skerbele and Lassetre [10] since our impact energy is 1500 eV. In fact, the maximum of  $v'=0$  of  $B^1\Sigma^+$  in this work is near  $K^2=0.25$  a.u., which is equal to the data of Chantranupong *et al.* [12], while it is 0.14 a.u. for Skerbele and Lassetre [10] at 300 and 400 eV, and 0.18 a.u. at 500 eV. Figure 5(b) shows the GOS versus  $K^2$  curves for  $v'=1$  of  $B^1\Sigma^+$ . Clearly, the profile of the calculated GOS curve [12] is similar to our result but the calculated data [12] are higher than those in this work except the data at  $0.5^\circ$  and  $1.0^\circ$ , which may be due to the large experimental errors and the finite acceptance angle for this transition in this work. The calculated maximum for  $v'=1$  of  $B^1\Sigma^+$  is 0.023 a.u., which is in agreement with our data.

Figures 5(c)–5(f) show the GOSs for  $v'=0-1$  of  $C^1\Sigma^+$  and  $E^1\Pi$ . Figure 5(c) shows that the present profile of  $v'=0$  of  $C^1\Sigma^+$  is similar to the theoretical result [12] although the absolute values are different. It is clear in Fig. 5(d) that there is a maximum for  $v'=1$  of  $C^1\Sigma^+$  and the

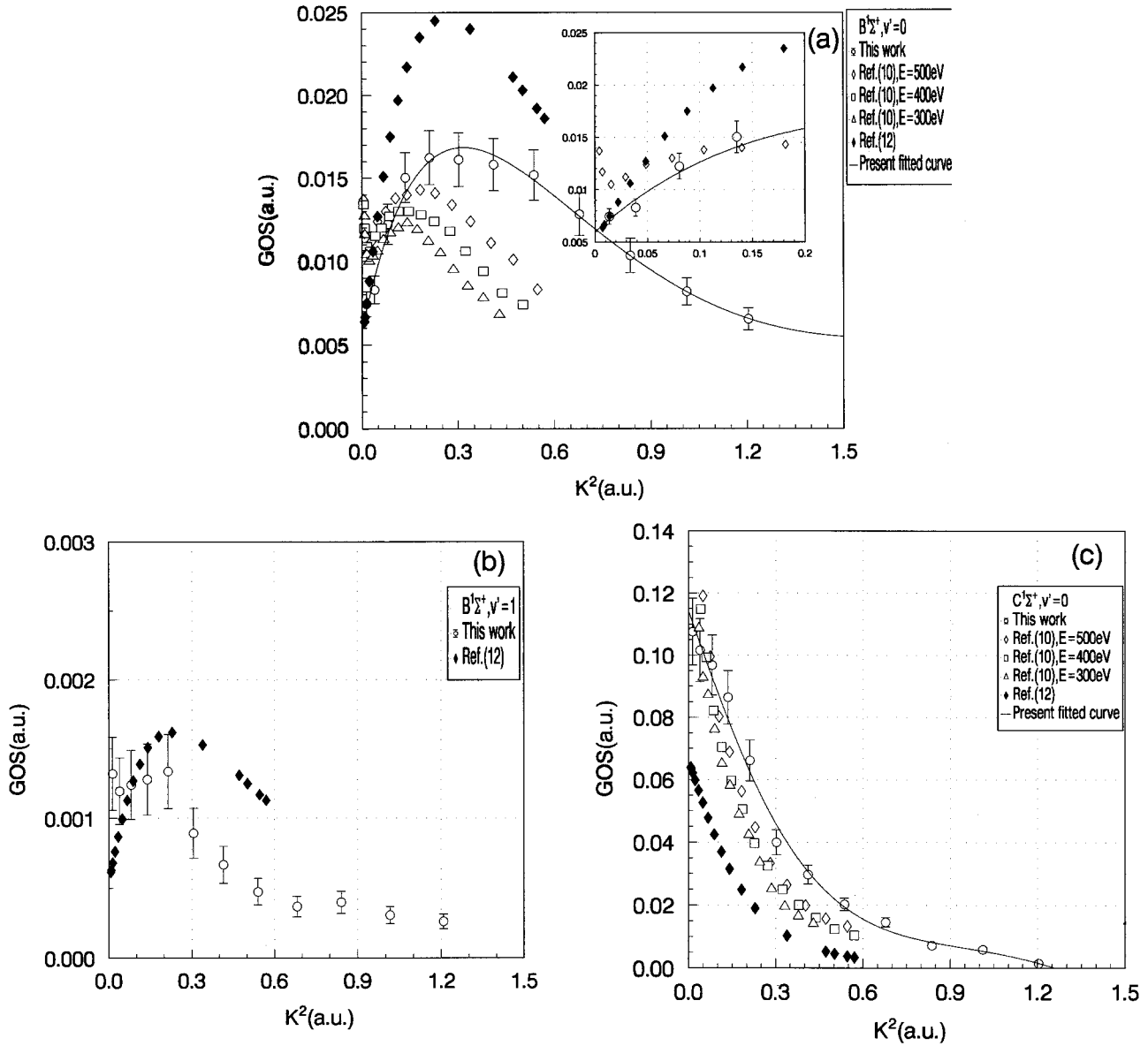


FIG. 5. (a) Absolute GOSs for  $v'=0$  of  $B^1\Sigma^+$  as a function of  $K^2$ . (b) Absolute GOSs for  $v'=1$  of  $B^1\Sigma^+$  as a function of  $K^2$ . (c) Absolute GOSs for  $v'=0$  of  $C^1\Sigma^+$  as a function of  $K^2$ . (d) Absolute GOSs for  $v'=1$  of  $C^1\Sigma^+$  as a function of  $K^2$ . (e) Absolute GOSs for  $v'=0$  of  $E^1\Pi$  as a function of  $K^2$ . (f) Absolute GOSs for  $v'=1$  of  $E^1\Pi$  as a function of  $K^2$ .

corresponding  $K^2$  are near 0.081 a.u. However, the theoretical calculations of Chantranupong *et al.* [12] show no maximum for  $v'=1$  of  $C^1\Sigma^+$ . Both the calculations [12] and our values show that there exists a minimum for  $v'=0$  of  $E^1\Pi$  shown in Fig. 5(e). However, our value of  $K^2$  (1.01 a.u.) of the minimum for  $v'=0$  of  $E^1\Pi$  is larger than the theoretical values (0.40 a.u.) [12]. It can be seen in Fig. 5(f) that there is a minimum ( $K^2=1.01$  a.u.) for  $v'=1$  of  $E^1\Pi$  in our measurement. However, the theoretical calculation [12] shows no minimum for the transition, but the largest calculated  $K^2$  is only 0.065 a.u.

The optical oscillator strengths for  $v'=0$  of  $B^1\Sigma^+$  and  $v'=0-1$  of  $C^1\Sigma^+$  and  $E^1\Pi$  by extrapolating the GOSs to  $K^2=0$  using Eq. (6) based on the above rules are shown in Table III. The estimated errors in experimental measurements are listed in parentheses including the error from extrapolating procedure. Clearly, the present values are consis-

tent with the data measured by Wu *et al.* [16] and Chan *et al.* [15] except that the data of  $v'=0$  of  $B^1\Sigma^+$ , but our values are smaller than the data of Lassette and Skerbele [9]. It has been indicated that the OOSs of Lassette and Skerbele [9] for  $v'=0$  of  $B^1\Sigma^+$ ,  $C^1\Sigma^+$ , and  $E^1\Pi$  were obtained from the ratios of the corresponding peaks to  $v'=2$  of  $A^1\Pi$  in zero angle spectrum according to Eq. (1) and normalized the relative data by the absolute OOS of  $v'=2$  of  $A^1\Pi$ . The OOSs for  $v'=0$  of  $B^1\Sigma^+$ ,  $C^1\Sigma^+$ , and  $E^1\Pi$ , which are obtained from our zero angle electron energy loss spectrum using Eq. (1) and the absolute OOS for  $v'=2$  of  $A^1\Pi$  as in the method of Lassette and Skerbele [9], are listed in Table III, they are larger than this work and the data measured by the dipole ( $e, e$ ) method, but close to the data of Lassette and Skerbele [9]. It indicates that the differences between the data of Lassette and Skerbele [9] and other data obtained by electron impact methods may be mainly due to the negli-

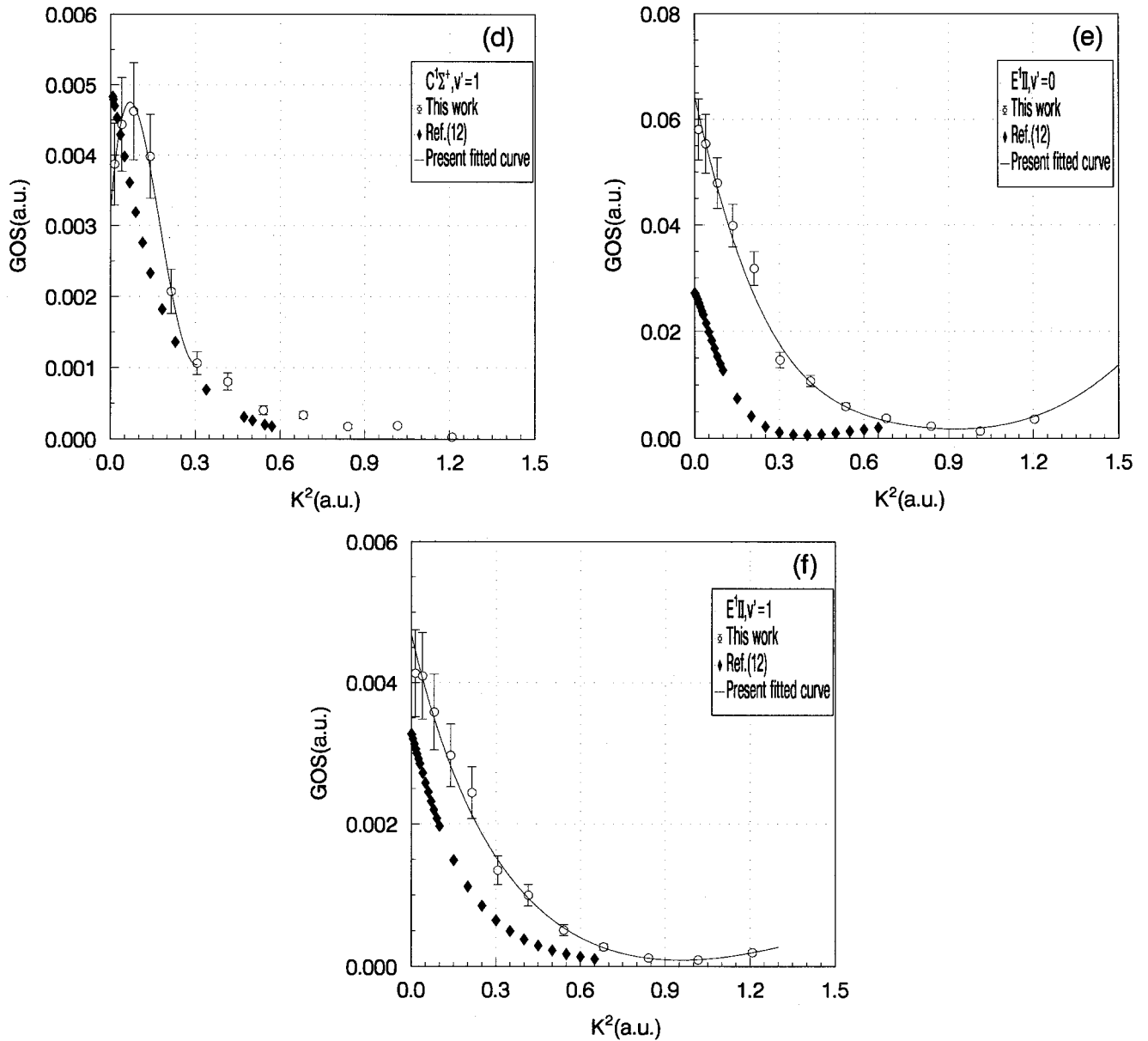


FIG. 5 (Continued).

gence of the finite acceptance angle at zero scattering angle measurement. In fact, we extrapolated the GOSs of  $v'=0$  of  $C^1\Sigma^+$  reported by Skerbele and Lassette [10] at 500 eV to  $K^2=0$  and obtained the limiting generalized oscillator strength of  $v'=0$  of  $C^1\Sigma^+$  at  $K^2=0$  is 0.13, which is consistent with the other electron impact results. For  $v'=0$  of  $B^1\Sigma^+$ , we have discussed above the reason why there is difference between this work and the data using the dipole ( $e, e$ ) method obtained by Wu *et al.* [16] and Chan *et al.* [15]. Although the present OOS of  $v'=0$  of  $B^1\Sigma^+$  is consistent with the value reported by Chantranupong *et al.* [11], the present OOSs of  $v'=0-1$  of  $C^1\Sigma^+$  and  $E^1\Pi$  show large deviations compared with the calculated values of Chantranupong *et al.* [11] and Kirby and Cooper [41]. Compared with optical measurements, there are also considerable discrepancies, as pointed out in Refs. [13,14]. Photoabsorption measurements based on Beer-Lambert law will be subject to so-called line saturation effect, especially for very sharp peaks with high cross section. It is clearly shown in

Table III that discrepancies of  $v'=0$  of  $C^1\Sigma^+$  and  $E^1\Pi$  are larger than that of small peaks of  $v'=0$  of  $B^1\Sigma^+$ ,  $v'=1$  of  $C^1\Sigma^+$  and  $E^1\Pi$  between the data of electron impact measurements and the data of photoabsorption measurements reported by Letzelter *et al.* [37].

#### IV. CONCLUSION

Absolute generalized oscillator strengths for the vibronic bands of  $A^1\Pi$ ,  $B^1\Sigma^+$ ,  $C^1\Sigma^+$ , and  $E^1\Pi$  at impact energy of 1500 eV and in the angle range of  $0.5^\circ$  to  $6.0^\circ$  have been measured in the present work. The experimental GOSs for  $v'=0-8$  of  $A^1\Pi$ ,  $v'=0-1$  of  $B^1\Sigma^+$  and  $C^1\Sigma^+$ , and  $E^1\Pi$  are reported. The present GOSs for  $v'=2$  of  $A^1\Pi$  are consistent with published experimental results [9] and theoretical values [12]. On the other hand, present profiles of GOS versus  $K^2$  curves for the  $B$ - $X$ ,  $C$ - $X$ , and  $E$ - $X$  transitions exhibit a similar appearance to the calculated curves of Chantranupong *et al.* [12], although these absolute GOS

TABLE III. The absolute optical oscillator strengths for  $v'=0-1$  of  $B^1\Sigma^+$ ,  $C^1\Sigma^+$ , and  $E^1\Pi(\times 10^{-2})$ .

	$B^1\Sigma_{v'=0}^+$	$C^1\Sigma_{v'=0}^+$	$C^1\Sigma_{v'=1}^+$	$E^1\Pi_{v'=0}$	$E^1\Pi_{v'=1}$
Experimental					
This work	0.598 (0.093)	11.4 (1.4)	0.322 (0.094)	6.42 (0.81)	0.467 (0.066)
a	1.11	18.1		9.35	
Wu <i>et al.</i> [16]	0.814	12.9	0.35	6.50	0.418
Chan <i>et al.</i> [15]	0.803	11.77	0.356	7.06	0.353
Lassette and Skerbele [9]	1.53	16.3		9.4	
Letzelter <i>et al.</i> [37]	0.45	6.19	0.28	3.65	0.25
Lee and Guest [38]	0.24	1.27		1.81	
Theoretical					
Chantranupong <i>et al.</i> [11]	0.508	6.47	0.49	2.74	0.329
Kirby and Cooper [41]	0.21	11.81	0.18	4.9	0.50

<sup>a</sup>The results obtained from our data at zero angle electron energy loss spectrum using the method of Lassette and Skerbele [9].

magnitudes show large differences compared with these calculated data [12]. This work and previous experimental data [10] show that GOS curves of  $v'=0$  of  $B^1\Sigma^+$  and  $C^1\Sigma^+$  fall on separate curves and GOSs become larger with increasing electron impact energy, which indicates that the first Born approximation does not hold for the two transitions at least up to the impact energy of 500 eV. With this in mind, one can expect that the calculated GOSs for  $B$ - $X$  and  $C$ - $X$  transitions including higher-order Born corrections may be closer to the present results. In addition, the positions of the maxima of  $v'=0-1$  of  $B^1\Sigma^+$  are in good agreement with the data of Chantranupong *et al.* [12], but the positions of the minima of  $v'=0$  of  $E^1\Pi$  are larger by a factor of 2 than the data of Chantranupong *et al.* [12]. We have found that the GOS versus  $K^2$  curve has a maximum at  $v'=1$  of  $C^1\Sigma^+$  and a minimum at  $v'=1$  of  $E^1\Pi$ .

Absolute optical oscillator strengths obtained by extrapolating the GOSs to  $K^2=0$  for the vibronic bands of  $A^1\Pi$ ,  $B^1\Sigma^+$ ,  $C^1\Sigma^+$ , and  $E^1\Pi$  are also reported. The present results have been compared with previous work. It is thought that the reason that the OOSs reported by Lassette and Skerbele [9] for the vibronic bands of  $B^1\Sigma^+$ ,  $C^1\Sigma^+$ , and  $E^1\Pi$  are much larger than the data of other electron impact measurements is the negligence of the finite acceptance angle at zero scattering angle measurement. The present OOSs are consistent with the values obtained by the dipole ( $e,e$ ) method measured by Wu *et al.* [16] and Chan *et al.* [15] except for  $v'=0$  of  $B^1\Sigma^+$ , and it is reasonably thought that the OOSs of Lassette and Skerbele [9] for the vibronic bands of  $B^1\Sigma^+$ ,  $C^1\Sigma^+$ , and  $E^1\Pi$  should be in agreement with other electron impact measurements if they took into

account the finite acceptance angle at zero scattering angle measurement. Therefore the data of the electron impact measurements are almost consistent with each other and the theory of limiting oscillator strength [20] at least has been verified in the case of carbon monoxide, because the OOSs obtained by two types of EELS methods are consistent except for  $v'=0$  of  $B^1\Sigma^+$ . The extrapolating EELS method may be tedious to determine the OOS of a transition, however, it provides the correct asymptotic behavior of GOS at small  $K^2$  of the transition. On the other hand, the limitation of the dipole ( $e,e$ ) method results from the finite acceptance angle and finite impact energy. Therefore for a transition in which the profile of the GOS curve is not similar to that of a dipole allowed transition at small  $K^2$ , the OOS obtained by the extrapolating EELS method may be more credible than that of the dipole ( $e,e$ ) method at the same impact energy, which is clearly shown in the case of  $v'=0$  of  $B^1\Sigma^+$  and in Refs. [24–26]. Although optical measurements [35,36] are in agreement with the present values and other electron impact measurements for the vibronic bands of  $A^1\Pi$ , there are considerable discrepancies between corresponding electron impact and optical measurements [37,38] for the vibronic bands of  $B^1\Sigma^+$ ,  $C^1\Sigma^+$ , and  $E^1\Pi$ , it may be partly due to the line-saturation effect in optical measurements.

## ACKNOWLEDGMENTS

Financial support for this work was provided by the National Natural Science Foundation of China and the National Education Committee of China. We also thank the University of Science and Technology of China for supporting this work.

[1] M. Inokuti, *Rev. Mod. Phys.* **43**, 297 (1971).

[2] R. A. Bonham, in *Electron Spectroscopy: Theory, Techniques and Applications*, edited by C. R. Brundle and A. D. Baker (Academic, New York, 1979), Vol. 3, p. 127.

[3] W. F. Chan, G. Cooper, and C. E. Brion, *Phys. Rev. A* **44**, 186 (1991).

[4] K. Z. Xu, R. F. Feng, S. L. Wu, Q. Ji, X. J. Zhang, Z. P. Zhong, and Y. Zheng, *Phys. Rev. A* **53**, 3081 (1996).

- [5] K. H. Sze, C. E. Brion, X. M. Tong, and J. M. Li, *Chem. Phys.* **115**, 433 (1987).
- [6] A. G. Middleton, M. J. Brunger, and D. J. O. Teubner, *J. Phys. B* **26**, 1743 (1993).
- [7] E. N. Lassette and S. M. Silverman, *J. Chem. Phys.* **40**, 1256 (1964).
- [8] V. D. Meyer, A. Skerbele, and E. N. Lassette, *J. Chem. Phys.* **40**, 1256 (1965).
- [9] E. N. Lassette and A. Skerbele, *J. Chem. Phys.* **54**, 1597 (1971).
- [10] A. Skerbele and E. N. Lassette, *J. Chem. Phys.* **55**, 424 (1971).
- [11] L. Chantranupong, K. Bhanuprakash, M. Honigmann, G. Hirsch, and R. J. Buenker, *Chem. Phys.* **161**, 351 (1992).
- [12] L. Chantranupong, G. Hirsch, K. Bhanuprakash, R. J. Buenker, M. Kimura, and M. A. Dillon, *Chem. Phys.* **164**, 183 (1992).
- [13] R. D. Hudson, *Rev. Geophys. Space Phys.* **6**, 305 (1971).
- [14] J. P. Bromberg, *J. Chem. Phys.* **52**, 1243 (1970).
- [15] W. F. Chan, G. Cooper, and C. E. Brion, *Chem. Phys.* **170**, 123 (1993).
- [16] S. L. Wu *et al.* (unpublished).
- [17] H. Bethe, *Ann. Phys. (Leipzig)* **5**, 325 (1930); *Z. Phys.* **76**, 293 (1932).
- [18] C. E. Brion and A. Hamnett, *Adv. Chem. Phys. Phys.* **45**, 1 (1981).
- [19] E. N. Lassette and A. Skerbele, in *Method of Experimental Physics*, edited by Dudley Williams, 2nd ed. (Academic Press, New York, 1974), Vol. 3, p. 892.
- [20] E. N. Lassette, A. Skerbele, and M. A. Dillon, *J. Chem. Phys.* **50**, 1829 (1969).
- [21] M. J. Van der Wiel, *Physica* **49**, 411 (1970).
- [22] M. J. Van der Wiel and G. Wiebes, *Physica* **53**, 225 (1971).
- [23] M. J. Van der Wiel and G. Wiebes, *Physica* **54**, 411 (1971).
- [24] S. L. Wu, Z. P. Zhong, R. F. Feng, S. L. Xing, B. X. Yang, and K. Z. Xu, *Phys. Rev. A* **51**, 4494 (1995).
- [25] Z. P. Zhong, S. L. Wu, R. F. Feng, S. L. Xing, B. X. Yang, Q. Ji, and K. Z. Xu (unpublished).
- [26] W. F. Chan, G. Cooper, X. Guo, and C. E. Brion, *Phys. Rev. A* **46**, 149 (1992).
- [27] R. F. Feng, B. X. Yang, S. L. Wu, S. L. Xing, F. Zheng, Z. P. Zhong, X. Z. Guo, and K. Z. Xu, *Sci. China A* **39**, 1288 (1996).
- [28] G. E. Chamberlain, J. A. Simpson, S. R. Mielczarek, and C. E. Kuyatt, *J. Chem. Phys.* **47**, 4266 (1967).
- [29] M. A. Dillon and E. N. Lassette, *J. Chem. Phys.* **62**, 2373 (1975).
- [30] Y. K. Kim and M. Inokuti, *Phys. Rev.* **175**, 176 (1968).
- [31] K. Z. Xu, Z. P. Zhong, S. L. Wu, R. F. Feng, S. Ohtani, T. Takayanagi, and A. Kimota, *Sci. China A* **38**, 368 (1995).
- [32] K. N. Klump and E. N. Lassette, *J. Chem. Phys.* **60**, 4830 (1974).
- [33] E. N. Lassette, *Can. J. Chem.* **47**, 1733 (1969).
- [34] M. Dillon, M. Kimuro, R. J. Suenker, G. Hirsch, Y. Li, and L. Chantranupong, *J. Chem. Phys.* **102**, 1561 (1995).
- [35] M. Eidelberg, F. Rostas, J. Breton, and B. Thieblemont, *J. Chem. Phys.* **96**, 5585 (1992).
- [36] R. W. Field, O. Benoist d'Azy, M. Lavollee, R. Lopez-Delgado, and A. Tramer, *J. Chem. Phys.* **78**, 2838 (1983).
- [37] C. Letzelter, M. Eidelberg, and F. Rostas, *Chem. Phys.* **114**, 273 (1987).
- [38] L. C. Lee and J. A. Guest, *J. Phys. B* **14**, 3415 (1981).
- [39] E. N. Lassette and A. Skerbele, in *Method of Experimental Physics*, (Ref. [19]), Vol. 3, p. 906.
- [40] J. F. Ying, C. P. Mathers, and K. T. Leung, *Phys. Rev. A* **47**, R5 (1993).
- [41] K. Kirby and D. L. Cooper, *J. Chem. Phys.* **90**, 4895 (1989).
- [42] E. N. Lassette, *J. Chem. Phys.* **53**, 3801 (1970).